Computational Mechanics 21 (1998) 512–525 © Springer-Verlag 1998

Large viscoplastic deformations of shells. Theory and finite element formulation

C. Sansour, F. G. Kollmann

Abstract The paper is concerned with large viscoplastic deformations of shells when the constitutive model is based on the concept of unified evolution equations. Specifically the model due to Bodner and Partom is modified so as to fit in the frame of multiplicative viscoplasticity. Although the decomposition of the deformation gradient in elastic and inelastic parts is employed, no use is made of the concept of the intermediate configuration. A logarithmic elastic strain measure is used. An algorithm for the evaluation of the exponential map for nonsymmetric arguments as well as a closed form of the tangent operator are given. On the side of the shell theory itself, the shell model is chosen so as to allow for the application of a three-dimensional constitutive law. The shell theory, accordingly, allows for thickness change and is characterized by seven parameters. The constitutive law is evaluated pointwise over the shell thickness to allow for general cyclic loading. An enhanced strain finite element method is given and various examples of large shell deformations including loading-unloading cycles are presented.

1 Introduction

Large strain viscoplastic deformations of thin structures occur very often in practical problems. Especially in metal forming processes the strains applied are finite and the structures under consideration are very thin. The application of shell theories to the modelling of such problems seems, accordingly, to be natural.

The aim of this paper is to give a formulation for finite strain viscoplastic deformations of shells under

- the application of the multiplicative decomposition of the deformation gradient into elastic and inelastic parts ([6, 24, 25]). The theoretical framework is casted in a general coordinate system well suited for shell problems.
- the use of a logarithmic-type strain measure.
- the employment of fully three-dimensional constitutive laws to allow for effects of cyclic loading.
- the use of constitutive equations of the unified type. Specifically a modified version of the Bodner & Partom model is considered.

Within the class of unified constitutive laws, time-dependent and time-independent effects are described by one and the same set of constitutive equations. Examples of such models can be found e.g. in Bodner & Partom [8], Chaboche [10], Krempl [23, 26], and Steck [43]. In this paper specifically a modified version of the Bodner & Partom model, the theoretical and numerical aspects of which are addressed by the authors in [36], is used. The theoretical setting is carried out in a coordinate-invariant form which allows for the application of arbitrary curvilinear coordinate systems.

Within unified constitutive equations the deformation is parameterized by the natural time parameter enabling the description of viscosity effects. This is entirely different from alternative theories such as the endochronic approach where the deformations are also parameterized by some scalar function not directly related to the real time scale. For such theories the reader is referred to Atluri [4] and Im and Atluri [17] who extended the original endochronic concept to include the case of finite strains.

As is well known the theory can be formulated in the material or in the spatial setting. For isotropic cases both formulations are completely equivalent. However, for anisotropic material behavior only the material formulation is adequate. In this paper we only consider isotropic material behavior. Since we want to formulate a theory which is open for an extension to anisotropy we apply the material formulation. Furthermore, we want to work with mixed tensors (contravariant-covariant strain-like quantities and covariant-contravariant stresses). Therefore, we introduce a mixed stress tensor in the reference configuration which is the pullback of Kirchhoff's stress tensor. Obviously this material stress tensor in nonsymmetric. It has to be observed that this nonsymmetry is only the result of a geometric transformation and does not reflect any physical features. We think that the constitutive formulation presented in this paper leaves the possibility to extend it to anisotropy where specific modifications may prove necessary.

In recent years considerable developments in the formulation of so-called geometrically exact shell formulations have been achieved (see e.g. [3, 5, 11, 33, 34, 40, 45]). Although different strain measures are used, a common

Communicated by S. N. Atluri, 03 February 1998

C. Sansour, F. G. Kollmann
Darmstadt University of Technology, Fachgebiet Maschinenelemente und Akustik, Magdalenenstr. 4, 64289 Darmstadt, Germany

Correspondence to: F. G. Kollmann

Dedicated to Professor P. Haupt, Kassel, on occasion of his 60th birthday

This research has been performed in Sonderforschungsbereich 298. Financial support of the Deutsche Forschungsgemeinschaft, Bonn-Bad Godesberg, is greatefully acknowledged.

feature within these formulations is the use of a rotation and the employment of the plane-stress assumption. Within physically linear computations efficient and robust finite elements has been developed. Hybrid stress, assumed strain, enhanced strain as well as the B-bar methods are able to prevent locking phenomena while preserving element stability.

For large strain formulations, the plane-stress assumption is too restrictive and the use of a rotation tensor may render the formulation complicated. Recently different approaches have been developed to make the shell formulation, on the one hand, capable for the application of a three-dimensional constitutive law and, on the other hand, to simplify the formulation itself while retaining the feature of being geometrically exact. For dropping the plane-stress assumption, the change of the shell thickness must be adequately considered. A shell theory with six degrees of freedom takes constant thickness change into account but proves to behave to stiffly. There are two ways to overcome this deficiency. Within the first one, the shortcoming of the theory is removed at the level of the numerical discretization. Here, the enhanced strain concept (Büchter et al. [9]) and the concept of assumed strains (Park et al. [31], Betsch & Stein [7]) have been used successfully. Within an alternative approach, the mentioned shortcoming is removed at the level of the shell theory itself and independent of the discretization process. The shell formulation must then allow for a at least linear distribution of the transversal normal strains over the shell thickness. For this task to be achieved a seven parameter shell was recently formulated in Sansour [35] which proved very effective and robust. A different formulation is given in Dvorkin et al. [12] where the number of parameters describing thickness change effects equals the number of Gaussian integration points used for a numerical integration over the shell thickness.

In this paper the theory given in [35] is modified and developed further to be capable for handling finite strain viscoplastic deformations. The most important modification concerns the evaluation of the constitutive law. In order to be capable to follow cyclic loading, the constitutive law must be evaluated pointwise over the shell thickness. The computation of the resultant forces and moments as well as their linearization is carried out numerically by means of a numerical integration procedure over the shell thickness. The internal variables too are to be evaluated at every integration point over the shell thickness.

Theoretical and computational aspects of finite strain time-independent and time-dependent inelastic deformations have been considered in Argyris & Doltsinis [2], Simo [37], Weber & Anand [44], Moran et al. [29], Eterovic & Bathe [13], Peric & Owen [32], Simo [38], Simo & Miehe [41], Miehe & Stein [28], Hackenberg & Kollmann [14]. It should be mentioned, anyhow, that the finite element formulations so far are typically given for cartesian coordinates not well suited for shell computations.

Specifically in [44] and [13] the integration of the evolution equations was carried out using the exponential map allowing for an exact fulfillment of the incompressibility constraint of the inelastic deformation. In [32, 13, 28] the elastic constitutive law is assumed to depend on a logarithmic strain measure. In [36] it is shown that a systematic exploitation of the geometric setting of the problem leads to compact and closed forms of the tangent operator in both the continuum and the algorithmic case as well.

Whereas there exists an extensive literature dealing with small strain time independent inelastic shell deformations, far less publications deal either with finite rate independent or rate dependent inelatic deformations. Kollmann & Mukherjee [20] developed a general, geometrically linear theory of shells. Based on this theory Kollmann & Bergmann [21] implemented an axisymmetric hybrid strain element where Hart's inelastic constitutive model has been used. A family of mixed and hybrid finite elements for axisymmetric shells using the Bodner &Partom viscoplastic model is given in Kollmann et al. [22]. The mentioned constitutive law has been also recently considered within small strain deformation of shells (additive decomposition of strains) by Klosowski et al. [18]. Kleiber & Kollmann [19] have extended the Bodner & Partom model to damage and implemented it into the mixed finite shell element described in [22].

A very early attempt to a finite strain rate dependent shell formulation is due to Hughes & Liu [15, 16]. They use a degenerated shell element and apply an anisotropic viscoplastic model to solve an impressive number of examples. Recently, Dvorkin & Pantuso [12] considered the formulation of the assumed strain element for large time-independent plastic deformations of general shells. The special case of axisymmetric shell deformations under the Kirchhoff-type restriction is considered in Wriggers et al. [46]. For a first attempt in the development of a general shell theory for large viscoplastic deformations we refer to An & Kollmann [1].

The paper is organized as follows: In section 2 basics of the kinematics of an elastic-viscoplastic body are briefly reviewed. In section 3, and for the paper to be self contained, an outline of the theoretical framework is given. The elastic constitutive law as well as the employed evolution equations are discussed. In section 4 and 5 the shell theory and the corresponding principle of virtual work are presented. In section 6 computational aspects of an implicit time integration procedure are discussed. The time integration is carried out using the exponential map to allow for an exact fullfilment of the incompressibility condition of the inelastic deformations. Specifically the algorithmic tangent operator is derived in a closed form. A four-node finite element formulation is developed in section 7. The finite element is based on a nonlinear version of the enhanced strain concept as formulated in Simo & Rifai [42] and applied by them to linear problems.

Various numerical examples are presented demonstrating the applicability of the theoretical frame work and the finite element formulation. In addition, basic features of the constitutive model employed are made transparent by the examples presented.

2
Kinematics of the elastic-inelastic body

Let $\mathbf{F}$ be the deformation gradient corresponding to a deformation of a body $\mathscr{B}$, the actual configuration of which is denoted $\mathscr{B}_t$. The corresponding tangent spaces are denoted by $T_X\mathscr{B}$ and $T_x\mathscr{B}_t$ for any $\mathbf{X} \in \mathscr{B}$ and $\mathbf{x} \in \mathscr{B}_t$. $\mathbf{X}$,$\mathbf{x}$ are related by means of the point map $\boldsymbol{\varphi}$: $\boldsymbol{\varphi}\mathbf{X} = \mathbf{x}$ and we have $\mathbf{F}$ as the tangent of $\boldsymbol{\varphi}$. A point of departure for an inelastic formulation constitutes the multiplicative decomposition [6, 24, 25] of the deformation gradient into an elastic and an inelastic part

$$\mathbf{F} = \mathbf{F}_e\mathbf{F}_p \quad . \tag{1}$$

For metals, the above decomposition is accompanied with the assumption $\mathbf{F}_p \in SL^+(3,\mathbb{R})$ which reflects the incompressibility of the inelastic deformations, where $SL^+(3,\mathbb{R})$ denotes the special linear group with determinant equal one. The decomposition (1) is often accepted as equivalent with the introduction of an intermediate configuration. In contrast to this understanding we define

$$\mathbf{F}_p := T_X\mathscr{B} \to T_X\mathscr{B} \quad , \tag{2}$$

$$\mathbf{F}_e := T_X\mathscr{B} \to T_x\mathscr{B}_t \quad . \tag{3}$$

That is, the inelastic part of the deformation gradient is a map from $T_X\mathscr{B}$ into itself. It is, accordingly, a material tensor uniquely defined by the evolution equation of an appropriately defined material plastic rate.

The following right Cauchy-Green-type deformation tensors are defined

$$\mathbf{C} := \mathbf{F}^{\mathrm{T}}\mathbf{g}\mathbf{F} \quad , \tag{4}$$

$$\mathbf{C}_e := \mathbf{F}_e^{\mathrm{T}}\mathbf{g}\mathbf{F}_e \quad , \tag{5}$$

$$\mathbf{C}_p := \mathbf{F}_p^{\mathrm{T}}\mathbf{g}\mathbf{F}_p \quad . \tag{6}$$

The deformation gradient $\mathbf{F}$ is an element of the general linear group $GL^+(3,\mathbb{R})$ with positive determinant. Therefore, we can attribute to its time derivative a left and right rate

$$\dot{\mathbf{F}} = \mathbf{l}\mathbf{F} \quad , \tag{7}$$

$$\dot{\mathbf{F}} = \mathbf{F}\mathbf{L} \quad . \tag{8}$$

Both rates are mixed tensors (contravariant-covariant). They are related by means of the equation

$$\mathbf{L} = \mathbf{F}^{-1}\mathbf{l}\mathbf{F} \quad . \tag{9}$$

Geometrically, (9) is the pull-back of the mixed velocity gradient from the current configuration to the reference configuration, e.g. $\mathbf{L} = \boldsymbol{\varphi}^*(\mathbf{l})$.

Since $\mathbf{F}_p \in SL^+(3,\mathbb{R})$ we can define a right rate according to

$$\dot{\mathbf{F}}_p = \mathbf{F}_p\mathbf{L}_p \tag{10}$$

which proves more appropriate for a numerical treatment in a purely material context.

3
Constitutive models

3.1
General considerations

Let $\boldsymbol{\tau}$ be the Kirchhoff stress tensor. Consider the expression of the internal power

$$\mathscr{W} = \boldsymbol{\tau} : \mathbf{l} \quad , \tag{11}$$

where $\mathbf{l}$ is defined in (7) and the relation holds $\mathbf{a} : \mathbf{b} = \operatorname{tr} \mathbf{a}\mathbf{b}^{\mathrm{T}}$ for $\mathbf{a}, \mathbf{b}$ being second order tensors and tr denoting the trace operation. The expression is rewritten using material tensors as

$$\mathscr{W} = \boldsymbol{\Xi} : \mathbf{L}. \tag{12}$$

The comparison of (11) with (12) leads with the aid of (9) to the definition equation of the material stress tensor $\boldsymbol{\Xi}$:

$$\boldsymbol{\Xi} = \boldsymbol{\varphi}^*(\boldsymbol{\tau}) = \mathbf{F}^{\mathrm{T}}\boldsymbol{\tau}\mathbf{F}^{-\mathrm{T}} \quad . \tag{13}$$

The tensor Ξ is, accordingly, the mixed variant pull-back of the Kirchhoff tensor. It coincides with Noll's intrinsic stress tensor and determines up to a spherical part the Eshelby stress tensor. In addition, one can say it is a Mandel-like stress tensor, the later being defined with respect to the so-called intermediate configuration.

A common feature of unified inelastic constitutive models is the introduction of phenomenological internal variables. We denote a typical internal variable as $\boldsymbol{Z}$. Assuming the existence of a free energy function according to $\psi = \psi(\mathbf{C}_e, \mathbf{Z})$, the localized form of the dissipation inequality for an isothermal process takes

$$\begin{aligned}\mathscr{D} &= \boldsymbol{\tau} : \mathbf{l} - \rho_{\mathrm{ref}}\,\dot{\psi} \\ &= \boldsymbol{\Xi} : \mathbf{L} - \rho_{\mathrm{ref}}\,\dot{\psi} \geq 0,\end{aligned} \tag{14}$$

where ρ_{ref} is the density at the reference configuration.

Making use of the relation

$$\begin{aligned}\dot{\mathbf{C}}_e = {} & \mathbf{F}_p^{-\mathrm{T}}\mathbf{L}^{\mathrm{T}}\mathbf{C}\mathbf{F}_p^{-1} + \mathbf{F}_p^{-\mathrm{T}}\mathbf{C}\mathbf{L}\mathbf{F}_p^{-1} \\ & - \mathbf{F}_p^{-\mathrm{T}}\mathbf{L}_p^{\mathrm{T}}\mathbf{C}\mathbf{F}_p^{-1} - \mathbf{F}_p^{-\mathrm{T}}\mathbf{C}\mathbf{L}_p\mathbf{F}_p^{-1}\end{aligned} \tag{15}$$

one may derive

$$\dot{\psi} = 2\mathbf{C}\mathbf{F}_p^{-1}\frac{\partial\psi}{\partial\mathbf{C}_e}\mathbf{F}_p^{-\mathrm{T}} : (\mathbf{L} - \mathbf{L}_p) + \frac{\partial\psi}{\partial\mathbf{Z}}\dot{\mathbf{Z}}. \tag{16}$$

The insertion of (16) into (14) leads to

$$\begin{aligned}\mathscr{D} = {} & \left(\boldsymbol{\Xi} - 2\rho_{\mathrm{ref}}\mathbf{C}\mathbf{F}_p^{-1}\frac{\partial\psi(\mathbf{C}_e,\mathbf{Z})}{\partial\mathbf{C}_e}\mathbf{F}_p^{-\mathrm{T}}\right) : \mathbf{L} \\ & + 2\rho_{\mathrm{ref}}\mathbf{C}\mathbf{F}_p^{-1}\frac{\partial\psi(\mathbf{C}_e,\mathbf{Z})}{\partial\mathbf{C}_e}\mathbf{F}_p^{-\mathrm{T}} : \mathbf{L}_p \\ & - \rho_{\mathrm{ref}}\frac{\partial\psi(\mathbf{C}_e,\mathbf{Z})}{\partial\mathbf{Z}}\dot{\mathbf{Z}} \geq 0 \quad .\end{aligned} \tag{17}$$

By defining Y as the thermodynamical force conjugate to the internal variable $\mathbf{Z}$

$$Y := -\rho_{\mathrm{ref}}\frac{\partial\psi(\mathbf{C}_e,\mathbf{Z})}{\partial\mathbf{Z}} \quad , \tag{18}$$

and making use of standard thermodynamical arguments, from (17) follows the elastic constitutive equation

$$\begin{aligned}\boldsymbol{\Xi} &= 2\rho_{\mathrm{ref}}\mathbf{C}\mathbf{F}_p^{-1}\frac{\partial\psi(\mathbf{C}_e,\mathbf{Z})}{\partial\mathbf{C}_e}\mathbf{F}_p^{-\mathrm{T}} \\ &= 2\rho_{\mathrm{ref}}\mathbf{F}_p^{\mathrm{T}}\mathbf{C}_e\frac{\partial\psi(\mathbf{C}_e,\mathbf{Z})}{\partial\mathbf{C}_e}\mathbf{F}_p^{-\mathrm{T}}\end{aligned} \tag{19}$$

as well as the reduced local dissipation inequality

$$\mathscr{D}_p := \boldsymbol{\Xi} : \mathbf{L}_p + \mathbf{Y} \cdot \dot{\mathbf{Z}} \geq 0 \quad , \tag{20}$$

where (18) has been considered. $\mathscr{D}_p$ is the plastic dissipation function. From (20) follows as an essential result that the stress tensor $\boldsymbol{\Xi}$ and the plastic rate $\mathbf{L}_p$ are conjugate variables. Observe that the tensor $\mathbf{L}_p$ is defined in (10).

3.2
The elastic constitutive model

Further we assume that the elastic potential can be decomposed additively into one part depending only on the elastic right Cauchy-Green deformation tensor $\mathbf{C}_e$ and the other one depending only on the internal variable $\mathbf{Z}$

$$\psi = \psi_e(\mathbf{C}_e) + \psi_Z(\mathbf{Z}). \tag{21}$$

Defining the logarithmic strain measure

$$\boldsymbol{\alpha} := \ln \mathbf{C}_e, \quad \mathbf{C}_e = \exp \boldsymbol{\alpha} \tag{22}$$

and assuming that the material is elastically isotropic, one can prove that the relation holds

$$\mathbf{C}_e \frac{\partial \psi_e(\mathbf{C}_e)}{\partial \mathbf{C}_e} = \frac{\partial \psi_e(\boldsymbol{\alpha})}{\partial \boldsymbol{\alpha}}, \tag{23}$$

where $\psi_e(\boldsymbol{\alpha})$ is the potential expressed in the logarithmic strain measure $\boldsymbol{\alpha}$. The proof is given in the appendix. Equation (19) results then in

$$\boldsymbol{\Xi} = 2\rho_{\text{ref}} \mathbf{F}_p^{\mathrm{T}} \frac{\partial \psi_e(\boldsymbol{\alpha})}{\partial \boldsymbol{\alpha}} \mathbf{F}_p^{-\mathrm{T}} \quad . \tag{24}$$

Note that ψ_e is an isotropic function of $\boldsymbol{\alpha}$. The last equation motivates the introduction of a modified logarithmic strain measure

$$\bar{\boldsymbol{\alpha}} := \mathbf{F}_p^{-1} \boldsymbol{\alpha} \mathbf{F}_p \quad . \tag{25}$$

Since the following relation for the exponential map holds

$$\mathbf{F}_p^{-1}(\exp \boldsymbol{\alpha})\mathbf{F}_p = \exp \bar{\boldsymbol{\alpha}} \quad , \tag{26}$$

(24) takes

$$\boldsymbol{\Xi} = 2\rho_{\text{ref}} \frac{\partial \psi(\bar{\boldsymbol{\alpha}})}{\partial \bar{\boldsymbol{\alpha}}} \quad . \tag{27}$$

It is interesting to note that (26) together with (22), (4), and (6) lead to a direct definition of $\bar{\boldsymbol{\alpha}}$. The relation holds

$$\bar{\boldsymbol{\alpha}} = \ln(\mathbf{C}_p^{-1}\mathbf{C}). \tag{28}$$

For computational simplicity a linear relation is assumed and therefore the elastic constitutive model (27) takes its final form

$$\boldsymbol{\Xi} = K \ \mathrm{tr}\ \bar{\boldsymbol{\alpha}}^{\mathrm{T}} \mathbf{1} + \mu \ \mathrm{dev}\ \bar{\boldsymbol{\alpha}}^{\mathrm{T}} \tag{29}$$

where

$$\bar{\boldsymbol{\alpha}}^{\mathrm{T}} = \ln(\mathbf{C}\mathbf{C}_p^{-1}), \tag{30}$$

and K is the bulk modulus and μ the shear modulus.

It should be stressed that the reduction of the elastic constitutive law to that given by (27) results in a considerable simplification of the computations necessary for the formulation of the weak form of equilibrium and its corresponding linearization. The only assumption we used was the very natural one of having an internal potential depending on $\mathbf{C}_e$. The following reduction is carried out systematically. The influence of the viscoplastic effects is completely captured in the well defined quantity $\mathbf{C}_p^{-1}$ which leads to a straightforward and very efficient numerical schemes as will be shown below.

3.3
Inelastic constitutive model

We make now use of the form of the inelastic constitutive model of Bodner and Partom [8]. In section 3.1 we concluded from (20) that the tensors $\boldsymbol{\Xi}$ and $\mathbf{L}_p$ are conjugate. A basic issue now is to put the mentioned constitutive model in a frame which stands in accord with this fact. Essentially we have to consider the stress tensor $\boldsymbol{\Xi}$ as the driving stress quantity while the plastic rate for which an evolution equation is to be formulated is taken to be $\mathbf{L}_p$. This leads to the following set of evolution equations

$$\mathbf{L}_p = \dot{\phi}\boldsymbol{\nu}^{\mathrm{T}} \quad , \tag{31}$$

$$\dot{Z} = \frac{M}{Z_0}(Z_1 - Z)\dot{W}_p \quad , \tag{32}$$

$$\begin{aligned} \dot{W}_p &= \Pi_{\mathrm{dev}\,\Xi}\dot{\phi}(\Pi_{\mathrm{dev}\,\Xi}, Z) \quad , \\ \Pi_{\mathrm{dev}\Xi} &= \sqrt{\tfrac{3}{2}\mathrm{dev}\,\boldsymbol{\Xi} : \mathrm{dev}\,\boldsymbol{\Xi}} \quad , \end{aligned} \tag{33}$$

$$\dot{\phi} = \frac{2}{\sqrt{3}} D_0 \exp\left[-\frac{1}{2}\frac{N+1}{N}\left(\frac{Z}{\Pi_{\mathrm{dev}\Xi}}\right)^{2N}\right] \quad , \tag{34}$$

$$\boldsymbol{\nu} = \frac{3}{2}\frac{\mathrm{dev}\boldsymbol{\Xi}}{\pi \mathrm{dev}\boldsymbol{\Xi}} \tag{35}$$

Here, Z_0, Z_1, D_0, N, M are material parameters. The choice of the transposed quantity in (31) is dictated by the resulting update formula for the stress tensor to be given in a following section. Moreover, the equation reflects the form given by associative viscoplasticity, when the classical flow functions are generalized and formulated in terms of nonsymmetric quantities.

Note that by its very definition in (13), the tensor $\boldsymbol{\Xi}$ is physically equivalent to the Kirchhoff stress tensor in the sense that both have the same invariants. The nonsymmetry of $\boldsymbol{\Xi}$ is a result of the geometric transformation from the actual to the reference configuration. Likewise, the skew-symmetric part of the rate $\mathbf{L}_p$ is of a purely geometric origin and can not be regarded as defining some kind of plastic spin. The forward transformation of $\mathbf{L}_p$ to the actual configuration results necessarily in a symmetric quantity.

In the case of isotropy under consideration, the issue of nonsymmetry of the stress tensor is irrelevant. Things may look different when anisotropic effects and kinematic hardening are considered. The topic of anisotropy is an active field of research with many open questions.

4
The shell theory

4.1
Preliminaries

We consider now coordinate charts ϑ^i which we take to be convected (attached to the body). For any $\mathbf{X} \in \mathscr{B}$ and $\mathbf{x} \in \mathscr{B}_t$ the tangent basis vectors at the reference and actual configurations are given by

$$\mathbf{G}_i = \mathbf{X}_{,i}, \quad \mathbf{g}_i = \mathbf{x}_{,i} \ , \tag{36}$$

where the relations hold $\mathbf{G}_i \cdot \mathbf{G}^j = \delta_i^j \cdot \mathbf{g}_i \cdot \mathbf{g}^j = \delta_i^j$. Here, derivatives with respect to ϑ^i are denoted by a comma, the scalar product of vectors by a dot, and δ_i^j is the Kronecker delta. The corresponding metrics at the actual and the reference configurations are denoted by $\mathbf{g}$ and $\mathbf{G}$, respectively. Their components are given by $G_{ij} = \mathbf{G}_i \cdot \mathbf{G}_j$ and $g_{ij} = \mathbf{g}_i \cdot \mathbf{g}_j$, respectively. The deformation gradient can be written down in terms of the basis vectors as

$$\mathbf{F} = \mathbf{g}_i \otimes \mathbf{G}^i \ . \tag{37}$$

For the construction of a shell theory a reference surface $\mathscr{M}$ is considered, which we will take to be the midsurface of $\mathscr{B}$. Following standards, the coordinate perpendicular to $\mathscr{M}, \vartheta^3$, will now be denoted by $z \in [-h/2, h/2], h \in \mathbb{R}$, and the tangent vectors of $\mathscr{T}\mathscr{M}$ in the undeformed reference configuration by $\mathbf{A}_\alpha (\alpha = 1, 2)$ and $\mathbf{N}$, with $\mathbf{N} \cdot \mathbf{A}_\alpha = 0$. We denote their images at an actual configuration by $\mathbf{a}_\alpha$ and $\mathbf{a}_3$, where in general $\mathbf{a}_3 \cdot \mathbf{a}_\alpha \neq 0$ and $|\mathbf{a}_3| \neq 1$. Thus we have $\mathbf{A}_\alpha = \mathbf{G}_\alpha|_{z=0}$ and $\mathbf{a}_\alpha = \mathbf{g}_\alpha|_{z=0}$. Further, $\mathbf{A}$ refers to the metric of the reference midsurface with covariant components $A_{\alpha\beta} = \mathbf{A}_\alpha \cdot \mathbf{A}_\beta$, $a_{\alpha\beta}$ are then the related components at the actual configuration. Their contravariant counterparts are denoted as usual by $A^{\alpha\beta}$ and $a^{\alpha\beta}$.

In addition to the curvilinear base vectors we consider the fixed cartesian frame $\boldsymbol{e}_i$ and define the quantities

$$c_{\alpha i} = \mathbf{A}_\alpha \cdot \mathbf{e}_i, \quad c_{3i} = \mathbf{N} \cdot \mathbf{e}_i \ , \tag{38}$$

to get the following relations

$$A_\alpha = c_{\alpha i}\mathbf{e}_i, \quad N = c_{3i}\mathbf{e}_i, \ \text{and} \ \mathbf{e}_i = c_{\alpha i}\mathbf{A}^\alpha + c_{3i}\mathbf{N} \tag{39}$$

which will be of use later on.

With $\mathbf{B}$ we denote the two-dimensional curvature tensor of the undeformed reference surface with components $B_{\alpha\beta} = -\mathbf{A}_\alpha \cdot \mathbf{N}_{,\beta}$. We also make use of the shifter tensor $\mathbf{J} = \mathbf{1} - z\mathbf{B}$. The exact expressions hold

$$\begin{aligned} \mathbf{G}_\alpha = \mathbf{A}_\alpha + z\mathbf{N}_{,\alpha} = (\mathbf{1} - z\mathbf{B})\mathbf{A}_\alpha = \mathbf{J}\mathbf{A}_\alpha, \\ \mathbf{G}^\alpha = \mathbf{J}^{-1}\mathbf{A}^\alpha, \quad \mathbf{G}_3 = \mathbf{N} \ . \end{aligned} \tag{40}$$

4.2 Shell strain measures

The shell theory is based on the following fundamental assumption. We assume that any configuration of the shell space is determined by the equation

$$\mathbf{x}(\vartheta^\alpha, z) = \mathbf{x}^0(\vartheta^\alpha) + (z + z^2\chi(\vartheta^\alpha))\mathbf{a}_3(\vartheta^\alpha) \ , \tag{41}$$

where $\mathbf{x}^0$ denotes a configuration of the midsurface. By that the ordered triple $(\mathbf{x}^0, \mathbf{a}_3, \chi)$ defines the configuration space of the shell.

The following basic features of the above assumption may be pointed out:

1. The assumed shell kinematics is the simplest possible which allows for a linear distribution of the transverse strains over the shell thickness. The constant part of transverse strains over the shell thickness is described by $\mathbf{a}_3$ whereas χ determines the linearly varying part. Note that the assumption is still valid: fibres perpendicular to the reference mid-surface remain straight after the deformation.
2. As a consequence of 1, three-dimensional constitutive equations can be applied. Accordingly, the formulation is suitable for small as well as for large strain cases in elasticity or elasto-viscoplasticity.
3. Without loss of accuracy in the limit case of thin shells, the use of a rotation tensor can be circumvented leading to a significant simplification of the whole shell formulation.

By $(36)_2$ and (41) the tangent vectors become

$$\begin{aligned} \mathbf{g}_\alpha &= \frac{\partial \mathbf{x}^0}{\partial \vartheta^\alpha} + (z + z^2\chi)\frac{\partial \mathbf{a}_3}{\partial \vartheta^\alpha} + z^2\frac{\partial \chi}{\partial \vartheta^\alpha}\mathbf{a}_3 \\ &= \mathbf{a}_\alpha + (z + z^2\chi)\mathbf{a}_{3,\alpha} + z^2\chi_{,\alpha}\mathbf{a}_3 \ , \end{aligned} \tag{42}$$

$$\mathbf{g}_3 = (1 + 2z\chi)\mathbf{a}_3 \ . \tag{43}$$

For the deformation gradient defined in (37) we may write

$$\begin{aligned} \mathbf{F} &= \mathbf{g}_\alpha \otimes \mathbf{G}^\alpha + \mathbf{g}_3 \otimes \mathbf{N} \\ &= \mathbf{a}_\alpha \otimes \mathbf{G}^\alpha + [(z + z^2\chi)\mathbf{a}_{3,\alpha} + z^2\chi_{,\alpha}\mathbf{a}_3] \otimes \mathbf{G}^\alpha \\ &\quad + (1 + 2z\chi)\mathbf{a}_3 \otimes \mathbf{N} \ . \end{aligned} \tag{44}$$

By defining the tangent map of the midsurface $\mathbf{F}^0 := \mathbf{F}|_{z=0}$

$$\mathbf{F}^0 := \mathbf{a}_\alpha \otimes \mathbf{A}^\alpha + \mathbf{a}_3 \otimes \mathbf{N} \ , \tag{45}$$

with $\mathbf{a}_\alpha = \mathbf{F}^0\mathbf{A}_\alpha, \mathbf{a}_3 = \mathbf{F}^0\mathbf{N}$ and by defining further the tensors

$$\mathbf{b} = \mathbf{a}_{3,\alpha} \otimes \mathbf{A}^\alpha + 2\chi\mathbf{a}_3 \otimes \mathbf{N} \ , \tag{46}$$

$$\mathbf{c} = (\chi\mathbf{a}_{3,\alpha} + \chi_{,\alpha}\mathbf{a}_3) \otimes \mathbf{A}^\alpha \ , \tag{47}$$

we arrive at the following expression for $\mathbf{F}$:

$$\mathbf{F} = (\mathbf{F}^0 + z\mathbf{b} + z^2\mathbf{c})\mathbf{J}^{-1} \ . \tag{48}$$

By introducing the displacement field $\mathbf{u}^0$ and the difference vector $\mathbf{w}$ according to

$$\mathbf{u}^0 := \mathbf{x}^0 - \mathbf{X}^0 \tag{49}$$

$$\mathbf{w} := \mathbf{a}_3 - \mathbf{N} \ , \tag{50}$$

with $\mathbf{X}^0$ defining a reference configuration of the midsurface, we get for (45)–(47)

$$\mathbf{F}^0 = (\mathbf{A}_\alpha + \mathbf{u}^0_{,\alpha}) \otimes \mathbf{A}^\alpha + (\mathbf{N} + \mathbf{w}) \otimes \mathbf{N} \ , \tag{51}$$

$$\mathbf{b} = -\mathbf{B} + \mathbf{w}_{,\alpha} \otimes \mathbf{A}^\alpha + 2\chi(\mathbf{N} + \mathbf{w}) \otimes \mathbf{N} \ , \tag{52}$$

$$\mathbf{c} = -\chi\mathbf{B} + [\chi\mathbf{w}_{,\alpha} + \chi_{,\alpha}(\mathbf{N} + \mathbf{w})] \otimes \mathbf{A}^\alpha \ . \tag{53}$$

Making use of (48), the right Cauchy-Green strain tensor of the shell space given in (4) takes the form

$$\begin{aligned} \mathbf{C} = \mathbf{J}^{-\mathrm{T}}[&\mathbf{F}^{0^\mathrm{T}}\mathbf{F}^0 + z(\mathbf{F}^{0^\mathrm{T}}\mathbf{b}) + \mathbf{b}^\mathrm{T}\mathbf{F}^0) \\ &+ z^2(\mathbf{b}^\mathrm{T}\mathbf{b} + \mathbf{F}^{0^\mathrm{T}}\mathbf{c} + \mathbf{c}^\mathrm{T}\mathbf{F}^0) \\ &+ z^3(\mathbf{b}^\mathrm{T}\mathbf{c} + \mathbf{c}^\mathrm{T}\mathbf{b}) + z^4\mathbf{c}^\mathrm{T}\mathbf{c}]\mathbf{J}^{-1}. \end{aligned} \tag{54}$$

The last expression motivates the definitions

$$\mathbf{C}^0 = \mathbf{F}^{0^\mathrm{T}}\mathbf{F}^0 \tag{55}$$

$$\mathbf{K} = \mathbf{F}^{0^\mathrm{T}}\mathbf{b} + \mathbf{b}^\mathrm{T}\mathbf{F}^0 \tag{56}$$

with the help of which we write for (54)

$$\mathbf{C} = \mathbf{J}^{-\mathrm{T}}[\mathbf{C}^0 + z\mathbf{K} + \cdots]\mathbf{J}^{-1}. \tag{57}$$

In what follows we assume that the shell is thin in the sense that the first two strain measures $\mathbf{C}^0$ and $\mathbf{K}$ are the dominant ones. The inclusion of all other strain measures is of course possible but is left out for the sake of simplicity.

We consider now the following decompositions

$$\mathbf{u}^0 = u_i\mathbf{e}_i, \;\; \mathbf{w} = w_i\mathbf{e}_i \tag{58}$$

$$\mathbf{C}^0 = C_{\alpha\beta}\mathbf{A}^\beta \otimes \mathbf{A}^\alpha + C_{3\alpha}A^\alpha \otimes \mathbf{N} + C_{\alpha3}\mathbf{N} \otimes \mathbf{A}^\alpha + C_{33}\mathbf{N} \otimes \mathbf{N}, \tag{59}$$

$$\mathbf{K} = K_{\alpha\beta}\mathbf{A}^\beta \otimes \mathbf{A}^\alpha + K_{3\alpha}A^\alpha \otimes \mathbf{N} + K_{\alpha3}\mathbf{N} \otimes \mathbf{A}^\alpha + K_{33}\mathbf{N} \otimes \mathbf{N}. \tag{60}$$

For the components of $\mathbf{C}^0$ and $\mathbf{K}$, (51), (52), (55) and (56) reveal the following expressions:

$$C_{\alpha\beta} = A_{\alpha\beta} + \mathbf{A}_\beta \cdot \mathbf{u}^0_{,\alpha} + \mathbf{A}_\alpha \cdot \mathbf{u}^0_{,\beta} + \mathbf{u}^0_{,\alpha} \cdot \mathbf{u}^0_{,\beta}, \tag{61}$$

$$C_{\alpha3} = \mathbf{N} \cdot \mathbf{u}^0_{,\alpha} + \mathbf{A}_\alpha \cdot \mathbf{w} + \mathbf{u}^0_{,\alpha} \cdot \mathbf{w}, \tag{62}$$

$$C_{3\alpha} = C_{\alpha3}, \tag{63}$$

$$C_{33} = 1 + 2\mathbf{N} \cdot \mathbf{w} + \mathbf{w} \cdot \mathbf{w}, \tag{64}$$

$$K_{\alpha\beta} = B_{\alpha\beta} + 2(\mathbf{N}_{,\alpha} \cdot \mathbf{u}^0_{,\beta} + \mathbf{N}_{,\beta}.\mathbf{u}^0_{,\alpha} + \mathbf{A}_\alpha \cdot \mathbf{w}_{,\beta} + \mathbf{A}_\beta \cdot \mathbf{w}_{,\alpha} + \mathbf{u}^0_{,\alpha} \cdot \mathbf{w}_{,\beta} + \mathbf{u}^0_{,\beta} \cdot \mathbf{w}_{,\alpha}) \;\; , \tag{65}$$

$$K_{\alpha3} = (\mathbf{N}_{,\alpha}.\mathbf{w} + \mathbf{N} \cdot \mathbf{w}_{,\alpha} + \mathbf{w}.\mathbf{w}_{,\alpha}) + 2\chi(\mathbf{A}_\alpha \cdot \mathbf{w} + \mathbf{N} \cdot \mathbf{u}^0_{,\alpha} + \mathbf{w} \cdot \mathbf{u}^0_{,\alpha}), \tag{66}$$

$$K_{33} = 4\chi(1 + 2\mathbf{N} \cdot \mathbf{w} + \mathbf{w} \cdot \mathbf{w}) \tag{67}$$

which are to be understood as the basic strain measures of the shell theory.

The finite element formulation to be given later on is carried out on the ground of the above strain measures in terms of cartesian components of $\mathbf{u}^0$ and $\mathbf{w}$ (Eq. 58). Explicitly we have:

$$C_{\alpha\beta} = A_{\alpha\beta} + c_{\beta i}u_{i,\alpha} + c_{\alpha i}u_{i,\beta} + u_{i,\alpha}u_{i,\beta}, \tag{68}$$

$$C_{\alpha3} = c_{3i}u_{i,\alpha} + c_{\alpha i}w_i + u_{i,\alpha}w_i, \tag{69}$$

$$C_{3\alpha} = C_{\alpha3}, \tag{70}$$

$$C_{33} = 1 + 2c_{3i}w_i + w_iw_i, \tag{71}$$

$$K_{\alpha\beta} = B_{\alpha\beta} + c_{3i,\alpha}u_{i,\beta} + c_{3i,\beta}u_{i,\alpha} + c_{\alpha i}w_{i,\beta} + c_{\beta i}w_{i,\alpha} + u_{i,\alpha}w_{i,\beta} + u_{i,\beta}w_{i,\alpha}, \tag{72}$$

$$K_{\alpha3} = (c_{3i,\alpha}w_i + c_{3i}w_{i,\alpha} + w_iw_{i,\alpha}) + 2\chi(c_{\alpha i}w_i + c_{3i}u_{i,\alpha} + wu_{i,\alpha}), \tag{73}$$

$$K_{33} = 4\chi(1 + 2c_{3i}w_i + w_iw_i). \tag{74}$$

Eqs. (68) to (74) are in fact quite compact expressions well suited for a numerical implementation.

5 The principle of virtual work

Let $\mathbf{S}$ be the second Piola-Kirchhoff stress tensor of the shell space.

The principle of virtual displacement in three-dimensions reads

$$\int_{\mathscr{B}} \frac{1}{2}\mathbf{S} : \delta\mathbf{C}\,\mathrm{d}V - \int_{\mathscr{B}} \mathbf{f} \cdot \delta\mathbf{x}\,\mathrm{d}V - \int_{\partial\mathscr{B}} \mathbf{t} \cdot \delta\mathbf{x}\,\mathrm{d}S = 0 \;\; , \tag{75}$$

where $\mathbf{f}, \mathbf{t}$ are the body and the surface forces, $\mathrm{d}V = J\,\mathrm{d}\sigma\,\mathrm{d}z$ (Naghdi [30]) with J denoting det $\mathbf{J}$, and $\mathrm{d}\sigma$ a surface element of the shell midsurface given by $\mathrm{d}\sigma = \sqrt{A}\,\mathrm{d}\vartheta^1\,\mathrm{d}\vartheta^2$, $A = \det(A_{\alpha\beta})$. We further assume that the shell midsurface $\mathscr{M}$ has a smooth curve $\partial\mathscr{M}$ as a boundary, with the parameter length s and the external normal vector $\boldsymbol{\nu}$. The boundary of the shell consists of three parts: an upper, a lower, and a lateral surface. If we denote the upper surface by $\partial\mathscr{B}^+$, the lower one by $\partial\mathscr{B}^-$ and the lateral one by $\partial\mathscr{B}^s$ and make use of the notation $J^+ = J|_{z=h/2}$, $J^- = J|_{z=-h/2}$, and J^s for J at the lateral surface, we may write for the surface elements $\mathrm{d}S^+ = J^+\,\mathrm{d}\sigma$, $\mathrm{d}S^- = J^-\,\mathrm{d}\sigma$ and $\mathrm{d}S^s = J^s\,\mathrm{d}z\,\mathrm{d}s$. First let us consider the external virtual work:

$$\delta\mathscr{W}_{\text{ext}} := \int_{\mathscr{B}} \mathbf{f} \cdot \delta\mathbf{x}\,\mathrm{d}V + \int_{\partial\mathscr{B}} \mathbf{t} \cdot \delta\mathbf{x}\,\mathrm{d}S \;\; , \tag{76}$$

With the definitions

$$\mathbf{p} := \int_{-h/2}^{h/2} \mathbf{f}J\,\mathrm{d}z + J^+\mathbf{t}^+ + J^-\mathbf{t}^- \;\; , \tag{77}$$

$$\mathbf{l} := \int_{-h/2}^{h/2} z\mathbf{f}J\,\mathrm{d}z + \frac{h}{2}J^+\mathbf{t}^+ - \frac{h}{2}J^-\mathbf{t}^- \;\; , \tag{78}$$

$$\mathbf{q} := \int_{-h/2}^{h/2} z^2\mathbf{f}J\,\mathrm{d}z + \frac{h^2}{4}J^+\mathbf{t}^+ + \frac{h^2}{4}J^-\mathbf{t}^- \;\; , \tag{79}$$

$$\mathbf{p}^s := \int_{-h/2}^{h/2} \mathbf{t}^sJ^s\,\mathrm{d}z \;\; , \tag{80}$$

$$\mathbf{l}^s := \int_{-h/2}^{h/2} z\mathbf{t}^sJ^s\,\mathrm{d}z \;\; , \tag{81}$$

$$\mathbf{q}^s := \int_{-h/2}^{h/2} z^2\mathbf{t}^sJ^s\,\mathrm{d}z \;\; , \tag{82}$$

Eq. (76) reduces to

$$\delta\mathscr{W}_{\text{ext}} := \int_{\mathscr{M}} [\mathbf{p} \cdot \delta\mathbf{x}^0 + (\mathbf{l} + \chi\mathbf{q}) \cdot \delta\mathbf{a}_3 + (\mathbf{q} \cdot \mathbf{a}_3)\delta\chi]\,\mathrm{d}\sigma + \int_{\partial\mathscr{M}} [\mathbf{p}^s \cdot \delta\mathbf{x}^0 + (\mathbf{l}^s + \chi\mathbf{q}^s) \cdot \delta\mathbf{a}_3 + (\mathbf{q}^s \cdot \mathbf{a}_3)\delta\chi]\,\mathrm{d}s \tag{83}$$

as the two-dimensional form of the external power.

To consider the internal virtual power we notice first that it is more appropriate to make use of the relation

$$\mathbf{S} = \mathbf{C}^{-1}\boldsymbol{\Xi} \tag{84}$$

since the inelastic constitutive model, as shown in section 3, is formulated in terms of $\boldsymbol{\Xi}$. We define first the pull-back of $\mathbf{S}$ under $\mathbf{J}$ which gives a stress tensor defined with respect to the midsurface

$$\mathbf{S}^0 = \mathbf{J}^{-1}\mathbf{C}^{-1}\boldsymbol{\Xi}\mathbf{J}^{-\mathrm{T}}. \tag{85}$$

Note that $\mathbf{S}^0$ is still z-dependent. Eqs. (57), (84) and (85) motivate the definitions

$$\mathbf{n} := \int_{-h/2}^{+h/2} \frac{1}{2}\mathbf{S}^0 J\,\mathrm{d}z = \int_{-h/2}^{+h/2} \mathbf{J}^{-1}\mathbf{C}^{-1}\frac{\partial\psi}{\partial\bar{\boldsymbol{\alpha}}}\mathbf{J}^{-\mathrm{T}} J\,\mathrm{d}z \qquad (86)$$

$$\mathbf{m} := \int_{-h/2}^{+h/2} z\mathbf{J}^{-1}\mathbf{C}^{-1}\frac{\partial\psi}{\partial\bar{\boldsymbol{\alpha}}}\mathbf{J}^{-\mathrm{T}} J\,\mathrm{d}z \qquad (87)$$

with the help of which as well as with (83), the principle of virtual power given in (75) takes the form

$$\begin{aligned}
&\int_{\mathscr{M}} [\mathbf{n} : \delta\mathbf{C}^0 + \mathbf{m} : \delta\mathbf{K}]\,\mathrm{d}\sigma \\
&\quad - \int_{\mathscr{M}} [\mathbf{p}\cdot\delta\mathbf{x}^0 + (\mathbf{1} + \chi\mathbf{q})\cdot\delta\mathbf{a}_3 + (\mathbf{q}\cdot\mathbf{a}_3)\delta\chi]\,\mathrm{d}\sigma \\
&\quad - \int_{\partial\mathscr{M}} [\mathbf{p}^s\cdot\delta\,\mathbf{x}^0 + (\mathbf{1}^s + \chi\mathbf{q}^s)\cdot\delta\mathbf{a}_3 \\
&\qquad\qquad + (\mathbf{q}^s\cdot\mathbf{a}_3)\delta\chi]\mathrm{d}s = 0 \ . \qquad (88)
\end{aligned}$$

For given external forces, the integrals (77)–(82) can be elaborated in almost closed form. For very thin shells the terms $\chi\mathbf{q}\cdot\delta\mathbf{a}_3, \mathbf{q}\cdot\mathbf{a}_3\delta\chi$ in (88) can be neglected as of being of higher order. Contrasting this, and in order to allow for the use of complex constitutive laws and path dependent behaviour (e.g. cyclic loading), the elaboration of (86) and (87) is carried out in practical computations numerically. That is, the constitutive equations are considered point-wise over the shell thickness.

6 Computational issues and time integration

In this section computational issues in conjunction with a possible finite element formulation are discussed. The time integration procedure of the constitutive model at hand is outlined and necessary operations of local iterations are discussed. A closed form of the algorithmic tangent operator is derived.

6.1 Time integration and local iteration

Let be given two discrete times t_n and t_{n+1} with time increment Δt. The understanding that the unimodular tensor $\mathbf{F}_\mathrm{P}$ is an element of the Lie group $SL^+(3,\mathbb{R}^3)$ while $\mathbf{L}_\mathrm{p}$ is an element of the corresponding Lie algebra motivates the use of the exponential map for time integration (see the introduction for the discussion of related work). We thus consider the following updating formula

$$\mathbf{F}_\mathrm{p}|_{n+1} = \mathbf{F}_\mathrm{p}|_n \exp[\Delta t\mathbf{L}_\mathrm{p}] \qquad (89)$$

for some $\mathbf{L}_\mathrm{p}$ in the interval Δt the choice of which is defined by means of the integration procedure. This algorithm preserves the condition of plastic incompressibility exactly.

The elastic strain measure $\mathbf{CC}_\mathrm{p}^{-1}$ at time step $n+1$ reads

$$\mathbf{CC}_\mathrm{p}^{-1}|_{n+1} = \mathbf{C}|_{n+1}\exp(-\Delta t\mathbf{L}_\mathrm{p})\mathbf{C}_\mathrm{p}^{-1}|_n \exp(-\Delta t\mathbf{L}_\mathrm{p}^\mathrm{T}) \qquad (90)$$

The plastic rate must be defined in accordance with the constitutive law under consideration. We make use of the predictor-corrector method according to which, at an iteration step i, the constitutive law is assumed first elastic defining the so called trial step. Within the plastic corrector step, the right Cauchy-Green tensor $\mathbf{C}$ is held fixed while $\mathbf{C}_\mathrm{p}$ is updated so as to fulfill the constitutive law.

We stipulate that $\mathbf{L}_\mathrm{p}$ is co-axial to $\boldsymbol{\Xi}_{n+1}^\mathrm{T}$ and therefore we choose

$$\mathbf{L}_\mathrm{p} = \dot{\phi}\boldsymbol{v}_{n+1}^\mathrm{T} \qquad (91)$$

for some $\dot{\phi}$ in the interval Δt. The value of the plastic rate $\dot{\phi}$ is so far undefined but it is constrained to assume a value within the time increment Δt in accord with the constitutive law at hand.

Due to the assumed isotropy of the problem (Eq. (29)), co-axiality of $\boldsymbol{\Xi}$ and $\bar{\boldsymbol{\alpha}}^T$ or of $\boldsymbol{\Xi}$ and $\mathbf{C}\mathbf{C}^{p^{-1}}$, respectively, holds. Thus, the single terms in the right hand side of (90) can be rearranged and the logarithm of the whole expression is the sum of the logarithm of the single terms:

$$\begin{aligned}
\ln(\mathbf{CC}_\mathrm{p}^{-1})_{n+1} &= \ln[\mathbf{C}_{n+1}\exp(-\Delta t\mathbf{L}_\mathrm{p})\mathbf{C}_\mathrm{p}^{-1}|_n \exp(-\Delta t\mathbf{L}_\mathrm{p}^\mathrm{T})], \\
&= \ln[\mathbf{C}_{n+1}\mathbf{C}_\mathrm{p}^{-1}|_n \exp(-2\Delta t\mathbf{L}_\mathrm{p}^\mathrm{T})], \qquad (92)\\
\bar{\boldsymbol{\alpha}}_{n+1}^\mathrm{T} &= (\bar{\boldsymbol{\alpha}}^\mathrm{trial})^\mathrm{T} - 2\Delta t\mathbf{L}_\mathrm{p}^\mathrm{T}.
\end{aligned}$$

Note that $(\bar{\boldsymbol{\alpha}}^\mathrm{trial})^\mathrm{T}$ defined as $\ln\mathbf{C}_{n+1}\mathbf{C}_\mathrm{p}^{-1}|_n$. A similar result for symmetric quantities defined with respect to the so called intermediate configuration is already obtained in [28].

In accord with the last relation the updating of the stress tensor has the form

$$\boldsymbol{\Xi}_{n+1} = \boldsymbol{\Xi}^\mathrm{trial} - \mu 2\Delta t\mathbf{L}_\mathrm{p}^\mathrm{T} \ , \qquad (93)$$

$$= \boldsymbol{\Xi}^\mathrm{trial} - 2\Delta t\,\dot{\phi}\,\mu\boldsymbol{v}_{n+1} \ . \qquad (94)$$

For some $\dot{\phi}$ in the corresponding interval. Note that $\boldsymbol{\Xi}^\mathrm{trial}$ is given as a function of $(\bar{\boldsymbol{\alpha}}^\mathrm{trial})^\mathrm{T}$.

From the definition of π in (33) and with the use of (94) we have

$$\Pi_{n+1} = \Pi^\mathrm{trial} - 3\Delta t\mu\,\dot{\phi} \ . \qquad (95)$$

We are now looking for the determination of $\dot{\phi}$ in consistency with (32)–(35) as well as with (95). In so doing we adopt the mid-point rule according to which we have

$$\Pi = \tfrac{1}{2}(\Pi_{n+1} + \Pi_n) = \tfrac{1}{2}(\Pi^\mathrm{trial} - 3\Delta t\mu\,\dot{\phi} + \Pi_n) \ , \qquad (96)$$

$$\dot{Z} = \frac{Z_{n+1} - Z_n}{\Delta t} \ , \qquad (97)$$

$$Z = \tfrac{1}{2}(Z_{n+1} - Z_n) \ . \qquad (98)$$

Inserting the last equations in (32), (33) we get, depending on $\dot{\phi}$, an explicit equation for the determination of the internal variable Z:

$$Z = \frac{m\Delta t\Pi\dot{\phi}Z_1 + 2Z_0 Z_n}{m\Delta t\Pi\dot{\phi} + 2Z_0}. \qquad (99)$$

Making use of this equation in the formulation for $\dot{\phi}$ (Eq. (34)):

$$\dot{\phi} = \frac{2}{\sqrt{3}} D_0 \exp\left[-\frac{1}{2}\frac{N+1}{N}\left(\frac{Z(\Pi,\dot{\phi})}{\Pi}\right)^{2N}\right] \tag{100}$$

and with (95) we get a nonlinear equation for the determination of $\dot{\phi}$. The equation is solved iteratively by the Newton-Raphson method. Note that $\dot{\phi}$ is a scalar function and not a rate. Therefore, it can be determined uniquely from (100).

6.2 The algorithmic tangent operator

With (94) at hand we can systematically derive the algorithmic tangent operator, which is given as the linearisation of $\mathbf{S}$ with respect to $\mathbf{C}$. One has first

$$\mathbf{S} = \mathbf{C}^{-1}(\Xi^{\text{trial}} - 2\Delta t\,\dot{\phi}\,\mu\boldsymbol{v}). \tag{101}$$

The derivative with respect to $\mathbf{C}$ gives

$$\begin{aligned}\frac{\partial\mathbf{S}}{\partial\mathbf{C}} &= \frac{\partial\mathbf{C}^{-1}}{\partial\mathbf{C}}(\boldsymbol{\Xi}^{\text{trial}} - 2\Delta t\,\dot{\phi}\,\mu\boldsymbol{v}) + \mathbf{C}^{-1}\frac{\partial\boldsymbol{\Xi}^{\text{trial}}}{\partial\mathbf{C}}\\ &\quad - 2\Delta t\mu\frac{\partial\dot{\phi}}{\partial\boldsymbol{\Pi}^{\text{trial}}}\frac{\partial\Pi^{\text{trial}}}{\partial\boldsymbol{\Xi}^{\text{trial}}}\frac{\partial\boldsymbol{\Xi}^{\text{trial}}}{\partial\mathbf{C}}\mathbf{C}^{-1}\boldsymbol{v}\\ &\quad - 2\Delta t\mu\dot{\phi}\mathbf{C}^{-1}\frac{\partial\boldsymbol{v}}{\partial\boldsymbol{\Xi}^{\text{trial}}}\frac{\partial\boldsymbol{\Xi}^{\text{trial}}}{\partial\mathbf{C}}\end{aligned} \tag{102}$$

We need now an expression for $\partial\dot{\phi}/\partial\boldsymbol{\Pi}^{\text{trial}}$ which depends on the employed constitutive law. We observe that $\dot{\phi}$ is to be understood as a function of Z as well as of Π. The same holds for Z which depends on $\dot{\phi}$ as well as on Π. On the other hand Π itself is, according to (95), a function of Π^{trial} and $\dot{\phi}$. Taking all this in consideration, (100) gives

$$\begin{aligned}\frac{\partial\dot{\phi}}{\partial\Pi^{\text{trial}}} &= \frac{\partial\dot{\phi}}{\partial\Pi}\left(\frac{\partial\Pi}{\partial\Pi^{\text{trial}}} + \frac{\partial\Pi}{\partial\dot{\phi}}\frac{\partial\dot{\phi}}{\partial\Pi^{\text{trial}}}\right)\\ &\quad + \frac{\partial\dot{\phi}}{\partial Z}\left(\frac{\partial Z}{\partial\Pi^{\text{trial}}} + \frac{\partial Z}{\partial\dot{\phi}}\frac{\partial\dot{\phi}}{\partial\Pi^{\text{trial}}}\right)\end{aligned} \tag{103}$$

which results in

$$\frac{\partial\dot{\phi}}{\partial\Pi^{\text{trial}}} = \frac{\frac{\partial\dot{\phi}}{\partial\Pi}\frac{\partial\Pi}{\partial\Pi^{\text{trial}}} + \frac{\partial\dot{\phi}}{\partial Z}\frac{\partial Z}{\partial\Pi^{\text{trial}}}}{1 - \frac{\partial\dot{\phi}}{\partial\Pi}\frac{\partial\Pi}{\partial\dot{\phi}} - \frac{\partial\dot{\phi}}{\partial Z}\frac{\partial Z}{\partial\dot{\phi}}} \tag{104}$$

Further, one has

$$\frac{\partial\Pi^{\text{trial}}}{\partial\boldsymbol{\Xi}^{\text{trial}}} = \boldsymbol{v}, \tag{105}$$

$$\frac{\partial(\boldsymbol{v})_i^j}{\partial(\boldsymbol{\Xi})_r^s} = -\frac{1}{\Pi}(\boldsymbol{v})_i^j(\boldsymbol{v})_s^r + \frac{3}{2\boldsymbol{\Pi}}\left(\delta_i^r\delta_s^j - \tfrac{1}{3}\delta_s^r\delta_i^j\right) \quad , \tag{106}$$

as well as

$$\begin{aligned}&\frac{\partial(\boldsymbol{\Xi}^{\text{trial}})_q^t}{\partial(\bar{\boldsymbol{\alpha}})_b^a}\frac{\partial(\bar{\boldsymbol{\alpha}})_b^a}{\partial(\mathbf{C})_{rs}}\\ &\quad = \left(K - \frac{1}{3}\mu(\mathbf{C}^{-1})^{rs}\delta_q^t + \mu(\mathbf{C}^{-1})^{rt}\delta_q^s\right) \quad .\end{aligned} \tag{107}$$

The last relation is proved in the appendix.

With the above results at hand we arrive for (102) at the very compact and closed form

$$\begin{aligned}\frac{\partial(\mathbf{S})_{ij}}{\partial(\mathbf{C})_{rs}} &= -(\mathbf{C}^{-1})^{ir}(\mathbf{C}^{-1})^{sk}[(\boldsymbol{\Xi}^{\text{trial}})_k^j - 2\Delta t\,\dot{\phi}\,\mu(\boldsymbol{v})_k^j]\\ &\quad + \beta_1(\mathbf{C}^{-1})^{ij}(\mathbf{C}^{-1})^{rs} + \beta_2(\mathbf{C}^{-1})^{is}\mathbf{C}^{-1})^{rj}\\ &\quad + \beta_3(\mathbf{C}^{-1})^{ik}(\boldsymbol{v})_k^j(\mathbf{C}^{-1})^{rt}(\boldsymbol{v})_t^s,\end{aligned} \tag{108}$$

where we have

$$\beta_1 = K - \frac{1}{3}\mu + \Delta t\mu^2\frac{\dot{\phi}}{\boldsymbol{\Pi}_{n+1}}, \tag{109}$$

$$\beta_2 = \mu - 3\Delta t\mu^2\frac{\dot{\phi}}{\boldsymbol{\Pi}_{n+1}}, \tag{110}$$

$$\beta_3 = -2\Delta t\mu^2\left(\frac{\partial\dot{\phi}}{\partial\boldsymbol{\Pi}^{\text{trial}}} - \frac{\dot{\phi}}{\boldsymbol{\Pi}_{n+1}}\right). \tag{111}$$

The relation (104) is to be used.

6.3 The exponential map with a nonsymmetric argument

As documented in (89), the updating of $\mathbf{F}_{\mathrm{P}}$ is carried out using the exponential map which insures the fullfillment of the incompressibility condition of the inelastic deformations. From (91) it is clear that the flow rule is formulated in terms of nonsymmetric quantities due to the fact that the stress tensor $\boldsymbol{\Xi}$ is nonsymmetric. In the literature, so far, the use of the exponential map was restricted to symmetric quantities and its evaluation was carried out by making use of the spectral decomposition. For nonsymmetric arguments the transformation to principal directions is not possible in general. In the following we give a general and simple algorithm for the evaluation of the exponential map with arbitrary arguments by exploiting the Cayley-Hamilton equation.

For any argument β, symmetric or not, we are concerned with the evaluation of $\exp\boldsymbol{\beta}$. Let I_1, I_2, I_3 be the invariants of $\boldsymbol{\beta}$ defined by the following equations

$$I_1 = \operatorname{tr}\boldsymbol{\beta} \quad , \tag{112}$$

$$I_2 = \tfrac{1}{2}(I_1^2 - \operatorname{tr}\boldsymbol{\beta}^2) \quad , \tag{113}$$

$$I_3 = \det\boldsymbol{\beta} \quad . \tag{114}$$

The Cayley-Hamilton equation gives

$$\boldsymbol{\beta}^3 = I_3\mathbf{1} - I_2\boldsymbol{\beta} + I_1^2 \quad . \tag{115}$$

The exponential map itself can be written as the following serie,

$$\exp\boldsymbol{\beta} = \mathbf{1} + \boldsymbol{\beta} + \frac{1}{2!}\boldsymbol{\beta}^2 + \frac{1}{3!}\boldsymbol{\beta}^3 + \frac{1}{4!}\boldsymbol{\beta}^4 + \cdots \tag{116}$$

On the other hand and since $\exp\boldsymbol{\beta}$ is an isotropic function of β the relation holds

$$\begin{aligned}\exp\boldsymbol{\beta} &= \alpha_0(I_1, I_2, I_3)\mathbf{1} + \alpha_1(I_1, I_2, I_3)\boldsymbol{\beta}\\ &\quad + \alpha_2(I_1, I_2, I_3)\boldsymbol{\beta}^2\end{aligned} \tag{117}$$

for $\alpha_0,\alpha_1,\alpha_2$ functions of the invariants of $\boldsymbol{\beta}$. The idea now is to compute the values of $\alpha_0,\alpha_1,\alpha_2$ in evaluating (116) by making successive use of (115).

For any power n one has first

$$\boldsymbol{\beta}^n = \gamma_0^{(n)}\mathbf{1} + \gamma_1^{(n)}\boldsymbol{\beta} + \gamma_2^{(n)}\boldsymbol{\beta}^2 \quad , \tag{118}$$

with $\gamma_0^{(n)},\gamma_1^{(n)},\gamma_2^{(n)}$ functions of the invariants of $\boldsymbol{\beta}$. Specifically for $n=3$ one has

$$\gamma_0^{(3)} = I_3, \quad \gamma_1^{(3)} = -I_2, \quad \gamma_2^{(3)} = I_1 \quad . \tag{119}$$

Starting from the last equation the functions $\gamma_0^{(n)}\gamma_1^{(n)},\gamma_2^{(n)}$ can be successively computed by making use of the relations

$$\gamma_0^{(n)} = I_3\gamma_2^{(n-1)} \quad , \tag{120}$$

$$\gamma_1^{(n)} = \gamma_0^{(n-1)} - I_2\gamma_2^{(n-1)} \quad , \tag{121}$$

$$\gamma_2^{(n)} = \gamma_1^{(n-1)} + I_1\gamma_2^{(n-1)} \quad , \tag{122}$$

the validity of which follows immediately from the Cayley-Hamilton equation.

The exponential map is now given by the evaluation of (117) where the comparison with (116) together with the last equations gives

$$\alpha_0 = 1 + \frac{1}{3!}I_3 + \sum_{n=4}^{N}\frac{1}{n!}\gamma_0^{(n)} \quad , \tag{123}$$

$$\alpha_1 = 1 - \frac{1}{3!}I_2 + \sum_{n=4}^{N}\frac{1}{n!}\gamma_1^{(n)} \quad , \tag{124}$$

$$\alpha_2 = \frac{1}{2} + \frac{1}{3!}I_1 + \sum_{n=4}^{N}\frac{1}{n!}\gamma_2^{(n)} \quad . \tag{125}$$

The number N is dictated by a desired accuracy up to which the exponential series is evaluated.

7
The finite element formulation

7.1
Interpolation of the geometry

The geometric quantities describing the shell surface (the fields $B_{\alpha\beta}, c_{\alpha i}, c_{3i}, \sqrt{A}$) are taken exactly at every integration point. The natural coordinates ϑ^α describing the shell surface are maped on the bi-unit square using bilinear interpolations.

On the other hand the cartesian components of the kinematical fields **u**, **w** as well as χ are interpolated using the bilinear interpolation functions. The same interpolations are taken for every Cartesian component of **u** and **w**.

7.2
An enhanced strain functional

We formulate first a strain-based element. In so doing we appeal to the enhanced strain concept in the spirit of Simo and Rifai [42] applied by them to linear problems. Accordingly the strain tensor itself is enhanced. This is contrasted with the nonlinear version of the concept as given by Simo and Armero [39] where the deformation gradient was enhanced. We consider accordingly the following functional

$$\frac{1}{2}\int_{\mathscr{B}}(\mathbf{C}+\mathbf{C}^{\mathrm{i}})^{-1}\boldsymbol{\Xi} : \delta(\mathbf{C}+\mathbf{C}^{\mathrm{i}})\,\mathrm{d}V - \int_{\mathscr{B}}\mathbf{f}\cdot\delta\mathrm{x}\,\mathrm{d}V - \int_{\partial\mathscr{B}}\mathbf{f}\cdot\delta\mathrm{x}\,\mathrm{d}S = 0 \quad . \tag{126}$$

where we have

$$\boldsymbol{\Xi} = 2\rho_{\mathrm{ref}}\frac{\partial\psi}{\partial\tilde{\boldsymbol{\alpha}}} = K\,\mathrm{tr}\,\tilde{\boldsymbol{\alpha}}^{\mathrm{T}}\mathbf{l} + \mu\left(\tilde{\boldsymbol{\alpha}}^{\mathrm{T}} - \frac{1}{3}\mathrm{tr}\,\tilde{\boldsymbol{\alpha}}^{\mathrm{T}}\mathbf{l}\right) \quad , \tag{127}$$

$$\tilde{\boldsymbol{\alpha}} = \ln[\mathrm{C}_{\mathrm{p}}^{-1}(\mathbf{C}+\mathbf{C}^{\mathrm{i}})] \tag{128}$$

and $\mathbf{C}^{\mathrm{i}}$ is the enhanced strain field. Since $\mathbf{C}^{\mathrm{i}}$ is assumed independent of the displacements, (126) splits into the two equations

$$\frac{1}{2}\int_{\mathscr{B}}(\mathbf{C}+\mathbf{C}^{\mathrm{i}})^{-1}\boldsymbol{\Xi} : \delta\mathbf{C}\,\mathrm{d}V - \int_{\mathscr{B}}\mathbf{f}\cdot\delta\mathbf{u}\,\mathrm{d}V - \int_{\partial\mathscr{B}_0}\mathbf{t}\cdot\delta\mathbf{u}\,\mathrm{d}S = 0 \tag{129}$$

and

$$\frac{1}{2}\int_{\mathscr{B}}(\mathbf{C}+\mathbf{C}^{\mathrm{i}})^{-1}\boldsymbol{\Xi} : \delta\mathbf{C}^{\mathrm{i}}\,\mathrm{d}V = 0 \quad . \tag{130}$$

The choice of the interpolation functions for $\mathbf{C}^{\mathrm{i}}$ is crucial in order to arrive at well behaving elements. First, we restrict $\mathbf{C}^{\mathrm{i}}$ to be of the form $\mathbf{C}^{\mathrm{i}} = \mathbf{J}^{-\mathrm{T}}\mathbf{C}^{0^{\mathrm{i}}}\mathbf{J}^{-1}$ where $\mathbf{C}^{0^{\mathrm{i}}}$ is independent of z. This is equivalent to an enhancement of the strains related to the shell midsurface alone.

These above equations are still defined for the three-dimensional shell body. The reduction to two dimensions is carried out in the same way as demonstrated in (77)–(88). One has

$$\begin{aligned}&\int_{\mathscr{M}}(\mathbf{n}:\delta\mathbf{C}^{\mathbf{0}} + \mathbf{m}:\delta\mathbf{K})\,\mathrm{d}\sigma \\ &\quad - \int_{\mathscr{M}}[\mathbf{P}\cdot\delta\mathbf{x}^{\mathbf{0}} + (\mathbf{l}+\chi\mathbf{q})\cdot\delta\mathbf{a}_3 + (\mathbf{q}\cdot\mathbf{a}_3)\delta\chi]\,\mathrm{d}\sigma \\ &\quad - \int_{\partial\mathscr{M}}\left[\mathbf{P}^s\cdot\partial\mathbf{x}^{\mathbf{0}} + (\mathbf{l}^s+\chi\mathbf{q}^s)\cdot\delta\mathbf{a}_3\right. \\ &\qquad\qquad \left. + (\mathbf{q}^s\cdot\mathbf{a}_3)\delta\chi\right]\mathrm{d}s = 0 \quad ,\end{aligned} \tag{131}$$

$$\int_{\mathscr{M}}\mathbf{n}:\delta\mathbf{C}^{0^{\mathrm{i}}}\,\mathrm{d}\sigma = 0 \quad . \tag{132}$$

The external load is defined in (77)–(82) while $\mathbf{n},\mathbf{m}$ are now defined according to

$$\mathbf{n} := \int_{-h/2}^{+h/2}\mathbf{J}^{-1}(\mathbf{C}+\mathbf{C}^{\mathrm{i}})^{-1}\frac{\partial\psi}{\partial\tilde{\alpha}}\mathbf{J}^{-\mathrm{T}}J\,\mathrm{d}z \tag{133}$$

$$\mathbf{m} := \int_{-h/2}^{+h/2}z\mathbf{J}^{-1}(\mathbf{C}+\mathbf{C}^{\mathrm{i}})^{-1}\frac{\partial\psi}{\partial\tilde{\alpha}}\mathbf{J}^{-\mathrm{T}}J\,\mathrm{d}z \quad . \tag{134}$$

The interpolation functions of the enhanced strains $\mathbf{C}^{0^{\mathrm{i}}}$ are taken to be of the form

$$C_{11}^i(\xi,\eta) = C_1\xi + C_2\xi\eta \tag{135}$$

$$C_{22}^i(\xi,\eta) = C_3\eta + C_4\xi\eta \tag{136}$$

$$C_{33}^i(\xi,\eta) = C_5\xi + C_6\eta + C_7\xi\eta \tag{137}$$

$$C_{12}^i(\xi,\eta) = C_8\xi + C_9\eta + C_{10}\xi\eta \tag{138}$$

$$C^i_{13}(\xi,\eta) = C_{11}\xi + C_{12}\xi\eta \tag{139}$$

$$C^i_{23}(\xi,\eta) = C_{13}\eta + C_{14}\xi\eta \ . \tag{140}$$

ξ and η are the local coordinates at the element level.

Clearly, the fields $C^i_{11}\dots C^i_{23}$ are the components of $\mathbf{C}^{0\mathrm{i}}$ with respect to the natural curvilinear base system $\mathbf{G}_i$.

The introduction of interpolation functions of the displacement fields as well as of the enhanced strain fields in (117) and (118) leads to two coupled nonlinear sets of algebraic equations. The enhanced strain field is assumed discontinuous over elements and is eliminated at the element level.

The linearization of (119) and (120) must be carried out numerically too. The tangent operator for the shell space given by (108) is a fourth order tensor which we denote by $\boldsymbol{H}$. The systematic linearisation of (119) and (120) leads to the following expressions

$$\begin{aligned}\int_{\mathscr{M}} [\Delta\mathbf{n} : \delta\mathbf{C}^0 + \Delta\mathbf{m} : \delta\mathbf{K}]\, \mathrm{d}\sigma &= \int_{\mathscr{M}} ([\boldsymbol{H}^0(\Delta\mathbf{C}^0 + \Delta\mathbf{C}^{0\mathrm{i}}) + \boldsymbol{H}^1\Delta\mathbf{K}] : \delta\mathbf{C}^0 \\ &\quad + [\boldsymbol{H}^1\Delta(\mathbf{C}^0 + \mathbf{C}^{0\mathrm{i}}) + \boldsymbol{H}^2\Delta\mathbf{K}] : \delta\mathbf{K}),\ \mathrm{d}\sigma \ ,\end{aligned} \tag{141}$$

$$\begin{aligned}\int_{\mathscr{M}} \Delta\mathbf{n} : \delta\mathbf{C}^{0\mathrm{i}}\, \mathrm{d}\sigma &= \int_{\mathscr{M}} ([\boldsymbol{H}^0(\Delta\mathbf{C}^0 + \Delta\mathbf{C}^{0\mathrm{i}}) \\ &\quad + \boldsymbol{H}^1\Delta\mathbf{K}] : \delta\mathbf{C}^{0\mathrm{i}})\, \mathrm{d}\sigma \ .\end{aligned} \tag{142}$$

The definitions hold

$$\begin{aligned}(\boldsymbol{H}^0)^{ijkl} :&= \int_{-h/2}^{+h/2} (\mathbf{J}^{-1})^i_a(\mathbf{J}^{-\mathrm{T}})^j_b(\boldsymbol{H})^{\mathrm{abrs}} \\ &\quad (\mathbf{J}^{-1})^k_r(\mathbf{J}^{-T})^l_s J\, \mathrm{d}z \ ,\end{aligned} \tag{143}$$

$$\begin{aligned}(\boldsymbol{H}^1)^{ijkl} :&= \int_{-h/2}^{+h/2} z(\mathbf{J}^{-1})^i_a(\mathbf{J}^{-\mathrm{T}})^j_b(\boldsymbol{H})^{\mathrm{abrs}} \\ &\quad (\mathbf{J}^{-1})^k_r(\mathbf{J}^{-T})^l_s J\, \mathrm{d}z \ ,\end{aligned} \tag{144}$$

$$\begin{aligned}(\boldsymbol{H}^2)^{ijkl} :&= \int_{-h/2}^{+h/2} z(\mathbf{J}^{-1})^i_a(\mathbf{J}^{-\mathrm{T}})^j_b(\boldsymbol{H})^{\mathrm{abrs}} \\ &\quad (\mathbf{J}^{-1})^k_r(\mathbf{J}^{-T})^l_s J\, \mathrm{d}z \ .\end{aligned} \tag{145}$$

The integral in (129)–(131) must be carried out numerically.

Further details of the implementation are standard and are hence omitted.

8
Numerical examples

We consider some numerical examples to illustrate the applicability of viscoplastic formulation as well as the shell theory to finite deformation shell problems. In all examples the following material data of titan as reported in [8] is considered:

$$\begin{aligned}K &= 123000\ \mathrm{N/mm^2}, \\ \mu &= 44000\ \mathrm{N/mm^2}, \\ D_0 &= 10000\ 1/\mathrm{sec}, \\ Z_0 &= 1150\ \mathrm{N/mm^2}, \\ Z_1 &= 1400\ \mathrm{N/mm^2}, \\ N &= 1, \\ M &= 100.\end{aligned}$$

8.1
Pinched cylinder with free edges

A cylinder with free edges is subject to two opposite point loads at the top and the bottom. The problem is described in Fig. 1. Making use of symmetry conditions only one-eighth of the cylinder is modeled using 20×30 elements. The depicted curves, given in Fig. 2, are those for the vertical displacement at the top and for the horizontal displacement at the side of the cylinder. The computation is carried out displacement-controlled with a time step $\Delta T = 1.0$ sec and for altogether 140 time steps. The load history is chosen so as to correspond to a linearly increasing displacement at the side of the cylinder until a maximum is arrived and then to a linearly decreasing displacement at the same point until the mentioned displacement vanishes. In both directions the deformation velocity is 1 mm/sec.

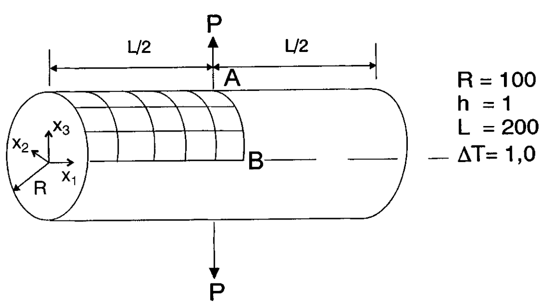

Fig. 1. Pinched cylinder with free edges. Problem definition

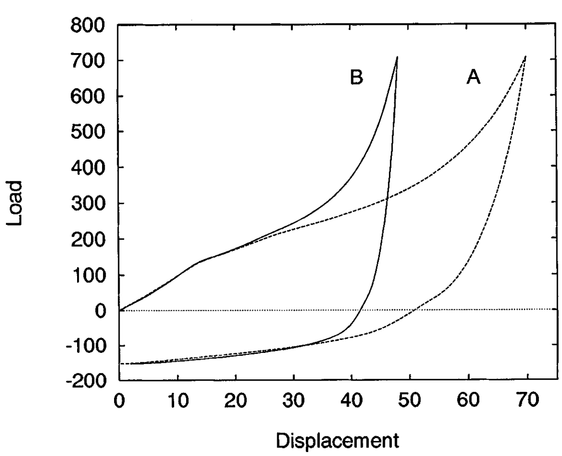

Fig. 2. Pinched cylinder with free edges. Load-displacement curve

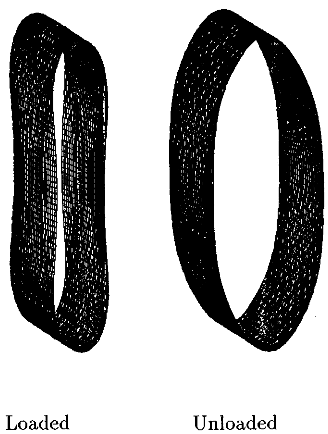

Fig. 3. Pinched cylinder with free edges. Deformed configurations

In Fig. 3 the configuration of the cylinder corresponding to maximum deformation is given. Also given is an unloaded configuration corresponding to a vanishing external loading.

8.2
Pinched cylinder with rigid diaphragm

The cylinder with rigid diaphragms is loaded by a line load acting in the x_3 direction at a segment of length of $0.25R\pi$. The problem is described in Fig. 4. Making use of symmetry conditions only one-eighth of the cylinder is modeled using 32×32 elements. The depicted curves (Fig. 2.2) are those of the vertical displacement at the top (point A) as well as of the horizontal displacement at the side of the cylinder (point B). The load history corresponding to a case of loading/unloading/negative-loading is chosen so as to result in a linearly increasing/linearly decreasing displacement at the top with a deformation velocity of 1 mm/sec. The time step used is 0.5 sec and altogether 400 time steps are computed.

Specifically, a vanishing displacement at point A does not correspond to a vanishing displacement at point B. Moreover, the latter displacement changes even sign. Within the last 10 time steps the displacement of point A is frozen. Relaxation effects take then place as slightly indicated in the plot.

In addition, the vertical displacement of point A corresponding to a solution of only 24×24 elements is included in Fig. 5. Qualitatively the response of the shell is still well captured, although the solution is clearly stiffer than that of the fine mesh.

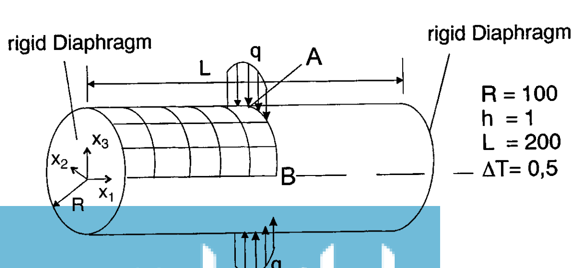

Fig. 4. Pinched cylinder with rigid diaphragm. problem definition

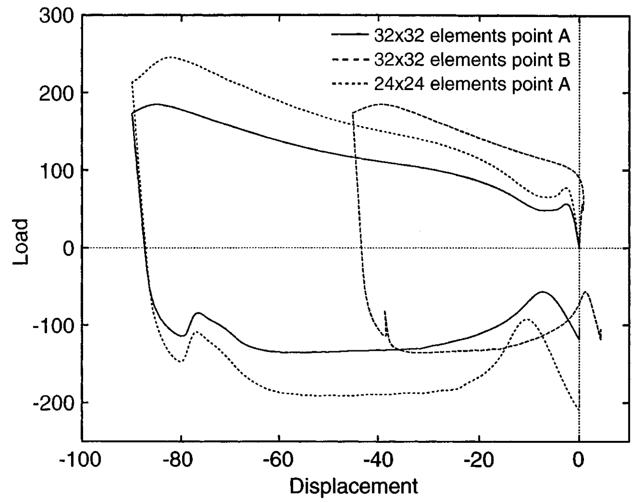

Fig. 5. Pinched cylinder with rigid diaphragm. Load-displacement curves

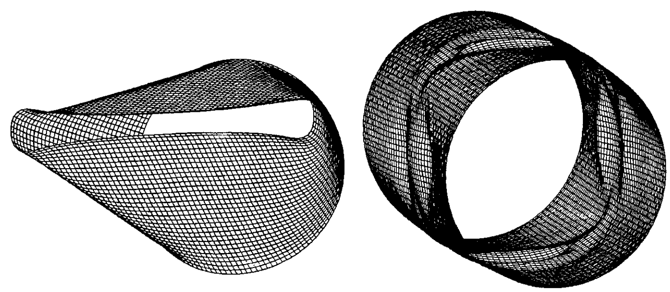

Fig. 6. Pinched cylinder with rigid diaphragm. Deformed configurations

A configuration corresponding to a maximum deformation of the cylinder is given in Fig. 6 (half cylinder). We note that the unloaded configuration exhibits only minor relaxation in comparison with the loaded one. In addition the final arrived deformed configuration is given in Fig. 3 as well.

8.3
Pinched hemispherical shell

The problem configuration is defined in Fig. 7. The sphere is subject to the action of two pairs of line loading in the x-

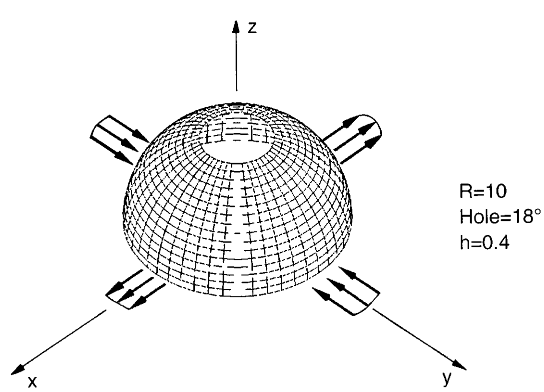

Fig. 7. Pinched hemispherical shell. Problem definition

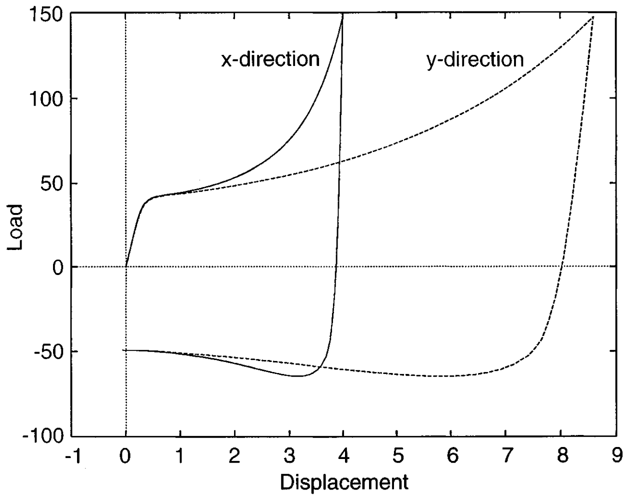

Fig. 8. Pinched hemispherical shell. Load-displacement curves

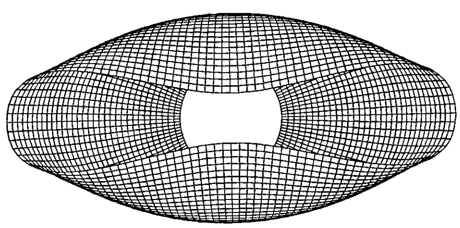

Fig. 9. Pinched hemispherical shell. Deformed configuration

and y-directions. The segment at each part of the loading has a length of $0.25R\pi$. Here one-quarter of the shell is modeled using 32×32 elements. The plots show the response at the points on the coordinate axes in both directions. The computation is carried out displacement-controlled with a time step of $\Delta T = 0.1$ sec. Taking the deformation at the point on the x-coordinate axes as a reference and choosing the velocity of that point to be 0.4 mm/sec, the deformation is linearly increased for 100 time steps and then decreased in the same manner for further 100 time steps. The corresponding load- displacement curves are given in Fig. 8. The maximal deformed configuration is given in Fig. 9.

9 Conclusion

In this paper a theory of shells including thickness change has been applied for finite strain viscoplastic deformations. The essential aspects of the formulation are

1. The finite strain theory of viscoplasticity is based on the multiplicative decomposition of the deformation gradient and the use of a logarithmic-type strain tensor.
2. Inspite of the finite strain formulation with logarithmic strains, a closed form of the algorithmic tangent operator for an implicit time integration is achieved.
3. A general algorithm to compute the exponential map for nonsymmetric arguments is provided.
4. A modified version of the Bodner &Partom unified constitutive equations of viscoplasticity is employed.
5. The shell theory incorporates seven degrees of freedom and allows for the application of three-dimensional constitutive laws without any modifications.
6. The constitutive law and the evolution equations are evaluated pointwise over the shell thickness. The resultant stress and moment tensors as well as the corresponding tangent material tensors are achieved by means of a numerical integration process over the shell thickness.
7. An enhanced finite element formulation is developed. The results of several examples confirm the element formulation.

Further it is to be stressed that, although in all examples the finite element behaved very well, the stability of the enhanced strain formulation for nonlinear problems is still an open question.

A Appendix

Derivation of Equation (23)

the $\mathbf{1}$ is the second order unit tensor and $\underset{4}{\mathbf{I}}$ is the fourth order unit tensor.

We want to prove that

$$\frac{\partial\psi_e}{\partial\mathbf{C}_e} : \frac{\partial\mathbf{C}_e}{\partial\boldsymbol{\alpha}} = \mathbf{C}_e \frac{\partial\psi_e}{\partial\mathbf{C}_e} \quad . \tag{A.1}$$

Since $\mathbf{C}_e = \exp\boldsymbol{\alpha}$ from the Taylor series representation of the exponential map follows

$$\mathbf{C}_e = \mathbf{1} + \boldsymbol{\alpha} + \frac{\boldsymbol{\alpha}^2}{2!} + \frac{\boldsymbol{\alpha}^3}{3!} + \cdots \tag{A.2}$$

Considering (A.2) and the isotropy of the function ψ_e the left hand side of (A.1) takes

$$\begin{aligned}\frac{\partial\psi_e}{\partial\mathbf{C}_e} : \frac{\partial\mathbf{C}_e}{\partial\boldsymbol{\alpha}} &= \frac{\partial\psi_e}{\partial\mathbf{C}_e} : \underset{4}{\mathbf{I}} + \frac{1\partial\psi_e}{2\partial\mathbf{C}_e}\boldsymbol{\alpha}^{\mathrm{T}} + \frac{1}{2}\boldsymbol{\alpha}^{\mathrm{T}}\frac{\partial\psi_e}{\partial\mathbf{C}_e} + \frac{1}{3!}\frac{\partial\psi_e}{\partial\mathbf{C}_e}\boldsymbol{\alpha}^{2\mathrm{T}} \\ &\quad + \frac{1}{3!}\boldsymbol{\alpha}^{2\mathrm{T}}\frac{\partial\psi_e}{\partial\mathbf{C}_e} + \frac{1}{3!}\boldsymbol{\alpha}^{\mathrm{T}}\frac{\partial\mathbf{C}_e}{\partial\boldsymbol{\alpha}}\boldsymbol{\alpha}^{\mathrm{T}} + \cdots \\ &= \frac{\partial\psi_e}{\partial\mathbf{C}_e} + \boldsymbol{\alpha}^{\mathrm{T}}\frac{\partial\psi_e}{\partial\mathbf{C}_e} + \frac{1}{2!}\boldsymbol{\alpha}^{2\mathrm{T}}\frac{\partial\psi_e}{\partial\mathbf{C}_e} + \cdots \\ &= C_e^{\mathrm{T}}\frac{\partial\psi_e}{\partial\mathbf{C}_e} = \mathbf{C}_e\frac{\partial\psi_e}{\partial\mathbf{C}_e} \quad ,\end{aligned} \tag{A.3}$$

where the symmetry of $\mathbf{C}_e$ has been considered.

The derivative of the logarithmic strain tensor

Since our elastic strain tensor is taken to be the logarithmic one (Eq. (27)), at the latest when deriving the tangent operator, an expression for the derivative of the logarithmic strain tensor with respect to $\mathbf{C}$ is then needed. As far as the logarithmic strain tensor has been used this task was achieved either approximately using specific assumptions and limitations [13, 32], or by appealing to the spectral decomposition [28] which is in fact very complicated due to the dependence of the eigen vectors on the deformation itself. In the following we derive a very simple formula for the expression we are looking for which seems to be completely overlooked in the literature.

First we observe that the following general relation holds

$$\Xi = 2\rho_{\text{ref}}\mathbf{C}\frac{\partial\psi}{\partial\mathbf{C}} \quad . \tag{A.4}$$

On the other hand we have already proven the relation

$$\Xi = 2\rho_{\text{ref}}\frac{\partial\psi}{\partial\bar{\boldsymbol{\alpha}}} \quad . \tag{A.5}$$

Since ψ is function of $\bar{\boldsymbol{\alpha}}$ and via the latter a function of $\mathbf{C}$, the relation must hold

$$\Xi = 2\rho_{\text{ref}}\mathbf{C}\left(\frac{\partial\psi}{\partial\bar{\boldsymbol{\alpha}}} : \frac{\partial\bar{\boldsymbol{\alpha}}}{\partial\mathbf{C}}\right) \quad . \tag{A.6}$$

Due to (A.5) we have further

$$(\Xi)_i^j = (\mathbf{C})_{ik}\left((\Xi)_a^b\frac{\partial(\bar{\boldsymbol{\alpha}})_b^a}{(\mathbf{C})_{kj}}\right) \tag{A.7}$$

from which it follows

$$\frac{\partial(\bar{\boldsymbol{\alpha}})_b^a}{(\mathbf{C})_{ij}} = (\mathbf{C}^{-1})^{ia}\delta_b^j \quad . \tag{A.8}$$

This is a very remarkable relation. Although $\bar{\boldsymbol{\alpha}}$ does depend explicitly on $\mathbf{C}_{\text{p}}$, in formula (A.8) only $\mathbf{C}$ is explicitly involved. Moreover, the formula is extremely simple as compared with a derivation via the spectral decomposition theorem.

With the above relation at hand, and with

$$\frac{\partial(\Xi^{\text{trial}})_q^t}{\partial(\bar{\boldsymbol{\alpha}})_b^a} = (K - \tfrac{1}{3}\mu)\delta_a^b\delta_q^t + \mu\delta_a^t\delta_q^b \quad , \tag{A.9}$$

Eq. (107) follows immediately.

References

[1] **An Q, Kollmann FG** (1996) A general theory of finite deformation of viscoplastic thin shells. Acta Mech. 117:47–70

[2] **Argyris JH, Doltsinis JSt** (1979) On the large strain inelastic analysis in natural formulation. Part I. Quasistatic problems. Comp. Meth. Appl. Mech. Engrg 20:213–252

[3] **Atluri SN** (1984) Alternate stress and conjugate strain measures, and mixed variational formulations involving rigid rotations, for computational analyses of finitely deformed solids, with application to plates and shells- Part I: Theory. Computers and Structures 18:93–116

[4] **Atluri SN** (1986) An endochronic approach and other topics in small and finite deformation plasticity, in: Finite Elements in Nonlinear Mechanics, (Eds: P. Bergan, E. Stein, W. Wunderlich) Springer, 17–48

[5] **Basar Y, Ding Y, Krätzig WB** (1992) Finite rotation shell elements via mixed formulations. Comp. Mech. 10:289–306

[6] **Besseling JF** (1968) A thermodynamic approach to rheology. In: Parkus, H. and Seddov, L.I. (eds.): Irreversible Aspects of Continuum Mechanics. Wien: Springer

[7] **Betsch P, Stein E** (1995) An assumed strain approach avoiding artificial thickness straining for a non-linear 4-node shell element. Comm. Num. Meth. Engrg. 11:899–909

[8] **Bodner SR, Partom Y** (1975) Constitutive equations for elastic-viscoplastic strain-hardening materials. ASME, J. Appl. Mech. 42:385–389

[9] **Büchter N, Ramm E, Roehl D** (1994) Three-dimensional extension of non-linear shell formulations based on the enhanced assumed strain concept. Int. J. Num. Meth. Engrg. 37:2551–2568

[10] **Chaboche JL** (1989) Constitutive equations for cyclic plasticity and cyclic viscoplasticity. Int. J. Plasticity 5:247–302

[11] **Chroscielewski J, Makowski J, Stumpf H** (1992) Genuinely resultant shell finite elements accounting for geometric and material nonlinearity. Int. J. Num. Meth. Engrg. 35:63–94

[12] **Dvorkin EN, Pantuso D** (1995) Formulation of the MITCY shell element for finite strain elasto-plastic analysis. Comp. Meth. Appl. Mech. Engrg. 125:17–40

[13] **Eterovic AL, Bathe KJ** (1990) A hyperelastic-based large strain elasto-plastic constitutive formulation with combined isotropic-kinemtic hardening using the logarithmic stress and strain measures, Int. J. Num. Meth. Engrg. 30:1099–1115

[14] **Hackenberg HP, Kollmann FG** (1995) A general theory of finite inelastic deformation of metals based on the concept of unified constitutive models. Acta Mech. 110:217–239

[15] **Hughes JR, Liu WK** (1981) Nonlinear finite element analysis of shells: Part 1: Three-dimensional shells. Comp. Meth. Appl. Mech. Engrg. 26:333–362

[16] **Hughes JR, Liu WK** (1981) Nonlinear finite element analysis of shells: Part 1: Two-dimensional shells. Comp. Meth. Appl. Mech. Engrg. 27:167–181

[17] **Im S, Atluri SN** (1987) A study of two finite strain plasticity models: an internal time theory using Mandel's director concept, and a general isotropic/kinematic-hardening theory, Int. J. Plasticity 3:163–191

[18] **Klosowski P, Woznica K, Weichert D** (1995) Dynamics of elasto-viscoplastic plates and shells, Arch. Appl. Mech. 65:326–345

[19] **Kleiber M, Kollmann FG** (1993) A theory of viscoplastic shells including damage. Arch. Mech. 45:423–437

[20] **Kollmann FG, Mukherjee S** (1985) A general geometrically linear theory of inelatic thin shells. Acta Mech. 57:41–67

[21] **Kollmann FG, Bergmann V** (1990) Numerical analysis of viscoplastic axisymmetric shells, based on a hybrid strain finite element. Comp. Mech. 7:89–105

[22] **Kollmann FG, Cordts D, Hackenberg HP** (1991) A family of mixed and hybrid finite elements for the numerical analysis of viscoplastic shells of revolution. In: Wriggers, P., Wagner, W. (eds.): Nonlinear Computational Mechanics. Berlin: Springer

[23] **Nishiguchi I, Sham TL, Krempl E** (1988) A finite deformation theory of viscoplasticity based on overstress. part i: constitutive equations. J. Appl. Mech. 57:548–552

[24] **Kröner E** (1960) Allgemeine Kontinuumstheorie der Versetzungen und Eigenspannungen. Arch. Rat. Mech. Anal. 4:273–334

[25] **Lee EH** (1969) Elastic-plastic deformation at finite strains. ASME J. Appl. Mech. 36:1–6

[26] **Liu MCM, Krempl E** (1979) A uniaxial viscoplastic model based on total strain and overstress. J. Mech. Phys. Solids 27:377–391

[27] **Mandel J** (1973) Equations constitutives et directeurs dans les milieux plastiques et viscoplastiques. Int. J. Solids Structures 9:725–740

[28] **Miehe C, Stein E** (1992) A canonical model of multiplicative elasto-plasticity: Formulation and aspects of the numerical implementation. Eur. J. Mech., A/Solids 11:25–43

[29] **Moran B, Ortiz M, Shih CF** (1990) Formulation of implicit finite element methods for multiplicative finite deformation plasticity Int. J. Num. Meth. Engrg. 29:483–514

[30] **Naghdi PM** (1972) The theory of shells. In: S. Flügge (ed.): Handbuch der Physik VI/2. Berlin Heidelberg New York: Springer

[31] **Park HC, Chao C, Lee SW** (1995) An efficient assumed strain element model with six dof per node for geometri-

cally nonlinear shells. Int. J. Num. Meth. Engrg. 38:4101–4122
[32] **Peric D, Owen DRJ, Honnor ME** (1992) A model for finite strain elasto-plasticity based on logarithmic strains: computational issues. Comp. Meth. Appl. Mech. Engrg. 94:35–61
[33] **Sansour C, Bufler H** (1992) An exact finite rotation shell theory, its mixed variational formulation and its finite element implementation. Int. J. Num. Meth. Engrg. 34:73–115
[34] **Sansour C, Bednarczyk H** (1995) The Cosserat surface as a shell model, theory and finite-element formulation. Comp. Meth. Appl. Mech. Engrg. 120:1–32
[35] **Sansour C** (1995) A theory and finite element formulation of shells at finite deformations involving thickness change: Circumventing the use of a rotation tensor. Arch. Appl. Mech. 65:194–216
[36] **Sansour C, Kollmann FG** (1997) On theory and numerics of large viscoplastic deformation, Comp. Meth. Appl. Mech. Engrg. 146:351–369
[37] **Simo JC** (1988) A frame work for finite strain elastoplasticity based on maximum plastic dissipation and multiplicative decomposition: Part II. Computational aspects, Comp. Meth. Appl. Mech. Engrg. 68:1–31
[38] **Simo JC** (1992) Algorithms for static and dynamic multiplicative plasticity that preserve the classical return mapping schemes of infinitesimal theory, Comp. Meth. Appl. Mech. Engrg. 99:61– 112
[39] **Simo JC, Armero F** (1992) Geometrically nonlinear enhanced strain mixed methods and the method of incompatible mode. Int. J. Num. Meth. Engrg. 33:1413–1449
[40] **Simo JC, Fox DD** (1989) On stress resultant geometrically exact shell model. Part I: Formulation and optimal parametrization. Comp. Meth. Appl. Mech. Engrg. 72:267–304
[41] **Simo JC, Miehe C** (1992) Associative coupled thermoplasticity at finite strains: Formulation, numerical analysis and implementation. Comp. Meth. Appl. Mech. Engrg. 98:41–104
[42] **Simo JC, Rifai MS** (1990) A class of mixed assumed strain methods and the method of incompatible modes. Int. J. Num. Meth. Engrg. 29:1595–1638
[43] **Steck EA** (1985) A stochastic model for the high-temperature plasticity of metals, Int. J. Plast. 1:243–258
[44] **Weber G, Anand L** (1990) Finite deformation constitutive equations and a time integration procedure for isotropic, hyperelastic- viscoplastic solids. Comp. Meth. Appl. Mech. Engrg. 79:173–202
[45] **Wriggers P, Gruttmann F** (1993) Thin shell with finite rotations in Biot stresses: theory and finite element formulation. Int. J. Num. Meth. Engrg. 36:4027–4043
[46] **Wriggers P, Eberlein R, Gruttmann F** (1995) An axisymmetrical quasi-Kirchhoff-type shell element for large plastic deformations. Arch. Appl. Mech. 65:465–477